AIAA Propulsion and Energy Forum
July 9-11, 2018, Cincinnati, Ohio
2018 Joint Propulsion Conference

10.2514/6.2018-4725

Electrospray Mass Spectroscopy of a HAN-based Monopropellant

Mitchell J. Wainwright,[1]
Missouri University of Science and Technology, Rolla, Missouri, 65409

Joshua L. Rovey,[2]
University of Illinois Urbana-Champaign, Urbana IL, 61801

Shawn W. Miller,[3]
Boston College, Institute for Scientific Research, Chestnut Hill, MA, 02467

Benjamin D. Prince,[4]
Air Force Research Laboratory, Space Vehicle Directorate, Kirtland AFB, NM, 87117

and
Steven P. Berg[5]
University of Illinois Urbana-Champaign, Urbana IL, 61801

A mixture of [Emim][$EtSO_4$]-HAN is a potential propellant suitable in a multi-mode chemical-electric microtube-electrospray micropropulsion system. This paper reports experimental mass spectrum results for this liquid when electrosprayed in a 50 μm capillary emitter. Mass spectra from 0-600 amu were obtained over a variety of angles and flow rates from 2 pL/sec to 3 nL/sec in both cation and anion extraction mode. Effects of flow rate and angular orientation on the spectra agree well with literature. Results show at least three of the four monomer species are emitted, along with numerous other species, some of which have been identified. Results also show, for the first time, emission of both proton-transferred covalent species paired with both ionic species for HAN. Also, because the liquid is a mixture, swapping of anions and cations between constituents is observed. This swapping is most evident in anion mode, where numerous forms of HAN ([HNO_3], 2[HNO_3], 2[HA-H], and [HAN]) appear in the spectra attached with [$EtSO_4$]$^-$. Numerous peaks in the spectra remain unidentified, but are speculated to be impurities and fragments.

I. Introduction

HYDROXYLAMMONIUM nitrate (HAN)-based monopropellants are being explored for multi-mode spacecraft propulsion [1-16]. Multi-mode propulsion is the use of two or more integrated, yet fundamentally different propulsive modes on a single spacecraft. Recently proposed systems make use of a high-specific impulse, usually electric mode, and a high-thrust, usually chemical mode. This can be beneficial in two primary ways: an increase in mission flexibility [17-21], and the potential to design a more efficient orbital manuever [22-25]. An increase in mission flexibility is achieved due to the availability of the two differing propulsive maneuvers to the mission designer

[1] Graduate Research Assistant, Department of Mechanical and Aerospace Engineering Missouri University of Science and Technology, Rolla, Mo, 65409, and Student AIAA Member. mjwmv4@mst.edu
[2] Associate Professor, Department of Aerospace Engineering, 317 Talbot Laboratory, 104 South Wright St., AIAA Associate Fellow. rovey@illinois.edu
[3] Research Associate, Institute for Scientific Research, St Clement's Hall 402, 140 Commonwealth Ave, and Member AIAA.
[4] Research Chemist, Space Vehicles Directorate, 3550 Aberdeen Building 570 and Member AIAA
[5] Intelligence Community Post-doctoral Fellow, Department of Aerospace Engineering, Talbot Laboratory, 104 South Wright St., Member AIAA.

at any point during the mission. This allows for drastic changes to the mission thrust profile at virtually any time before or even after launch without the need to integrate an entirely new propulsion system. Additionally, it has been shown that under certain mission scenarios it is beneficial in terms of spacecraft mass savings, or deliverable payload, to utilize separate high-specific impulse and high-thrust propulsion systems even in hybrid propulsion systems [22, 24, 26]. However, even greater mass savings can be realized by using a shared propellant and/or hardware, even if the thrusters perform lower than state-of-the-art in either or both modes [4, 19]. In order to realize the full potential of a multi-mode propulsion system, it is necessary to utilize one shared propellant for both modes; this allows for a large range of possible maneuvers while still allowing for all propellant to be consumed regardless of the specific choice or order of maneuvers [20].

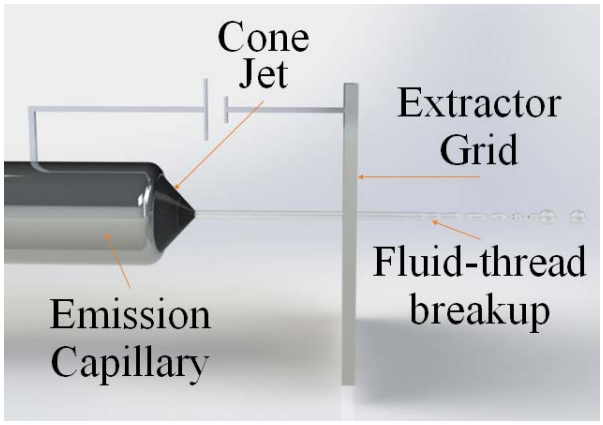

Figure 1: Illustration of capillary electrospray emission.

One promising approach to multi-mode propulsion integrates an electric electrospray thruster with a chemical microtube thruster, and this system has significant advantages in terms of flexibility and adaptability for small spacecraft [6, 8, 9]. Electrospray propulsion systems have already been selected for small spacecraft applications [27, 28], and chemical microtube thrusters have also been proposed for micropropulsion [29-32]. An electrospray thruster creates thrust through ion evaporation and electrostatic acceleration of ions and droplets from a liquid surface under applied electric field as shown in Figure 1. A microtube thruster is a heated tube with a typical diameter of 1 mm or less, and may have a catalytic surface material. These microtubes might also be used as the capillary type emitters in electrospray propulsion systems. This system would have one shared propellant tank, one set of feed lines and valves, and one thruster that can alternate between high thrust chemical microtube mode or high specific impulse electric electrospray mode. A major challenge for a multi-mode microtube-electrospray propulsion system is developing and demonstrating a propellant that can perform in both modes. Typical electrospray propulsion uses benign ionic liquid solvents that are not chemically reactive, such as [Emim][Im] and [Emim][BF_4] [33, 34], while chemical microtube propulsion uses traditional monopropellant liquids like hydrazine or gaseous propellants, such as hydrogen and oxygen [35-37], that are not electrosprayable.

Recent research has identified a promising monopropellant for a microtube-electrospray propulsion system.[4]. This propellant is a mixture of 1-ethyl-3-methylimidazolium ethyl sulfate ([Emim][EtSO4]) and hydroxylammonium nitrate (HAN) at a 59:41 HAN-[Emim][$EtSO_4$] ratio by mass. This mixture ratio has been optimized to provide chemical performance similar to other state-of-the-art monopropellants such as hydrazine, LMP-103, and AF-M315E (~250 sec theoretical with a nozzle). Theoretically it has a highly competitive density specific impulse of 354,750 kg-s/m^3 (compared with 365,000 kg-s/m^3 for AF-M315E), while also having a very desirable lower combustion temperature (1850 K vs. 2100 K) [4]. It has been theoretically investigated [3, 4], synthesized and shown to have good thermal and catalytic decomposition within a microreactor [2, 5, 7, 10], shown to have stable high performance in an electrospray emitter [11], and demonstrated burn rate similar to other HAN-based monopropellants.[15, 38].

HAN-[Emim][$EtSO_4$] propellant is different from traditional electrospray propellants. It is a double-salt ionic liquid (DSIL), whereas traditional propellants (e.g., [Emim][Im], [Emim][BF_4]) are neat ionic liquids (ILs). Ionic liquids are molten salts that are liquid at room temperature. Pure [HAN] is ionic and exists as a solid monoclinic salt at room temperature [39], but readily dissolves into [Emim][$EtSO_4$] creating a mixture of two salts or a double salt. DSILs are interesting in that their properties do not necessarily obey traditional mixing laws [40-48]. That is, mixtures of ILs can have properties, such as conductivity, density, and viscosity, which do not match simple mole or mass averaged values of the individual components. Inter-molecular interactions within the liquid can be indicative of what is emitted during electrospray and, conversely, electrospray emission may be an analog to internal interactions, thus allowing conclusions on how these salts are interacting within the liquid [49]. In other words, mass spectroscopy may be used to observe how the ions are interacting within a DSIL.

The mass spectra of emitted ions and droplets are well-known for electrospray of neat ILs,[49-51] but have not been studied extensively for DSILs, especially those with HAN. Lozano has studied the species and energies emitted by a single externally wetted needle with [Emim][BF_4] [52]. Miller et. al. have investigated the ion and droplet contribution in capillary electrospray of [Bmim][DCA] [53, 54], as well as an extensive investigation of [Emim] and [Bmim] cations paired with [Im], [DCA], and [BF_4] anions [55]. A few studies to electrospray mixtures are done by

Garoz and de la Mora [56], Guerrero et al. [57], and Garoz et al. [58]. Garoz and de la Mora have used time-of-flight for formamide and methylammonium formate mixtures and predicted propulsion performance [56]. Guerrero et al. have explored propylene carbonate mixtures with [Emim][Im] or [Emim][BF_4] and used time-of-flight measurements to predict propulsion performance [57]. Garoz et al. studied the properties of electrospray liquids that result in pure ion emission and focused on [Emim][$GaCl_4$], [Emim][$C(CN)_3$]. and [Emim][$N(CN)_2$] [58].

The focus of this work is on mass spectrometry of the DSIL propellant HAN-[Emim][$EtSO_4$]. Quadrupole mass spectrometry is used to identify the mass of ions emitted by a capillary emitter within the mass range 0 – 600 amu in both cation and anion emission modes. The goal is to compare and correlate observed ion masses with theoretically expected ion masses based on the species present within the liquid mixture.

II. Experimental Setup

A. HAN-[Emim][EtSO4] Propellant

The process for synthesizing the propellant is described in detail in previous studies [5, 7, 12]. The same synthesis path is used here, starting with raw 24% aqueous HAN (Sigma Aldrich) and >95% pure [Emim][$EtSO_4$] (Sigma Aldrich). The mixture ratio is 59:41 HAN-[Emim][$EtSO_4$] by mass, the density is 1.53 g/cc, and it has very low water content. A major challenge with multi-mode chemical-electrospray monopropellants is water content. Most HAN-based monopropellants have significant (~>10%) water content [16, 59-65]. Water is added to HAN-based propellants for two reasons. First it reduces the combustion temperature to a level below the melting and sintering point of typical catalyst materials. Second, it enhances the stability of the propellant. Specifically, the presence of polar water molecules creates a strong hydrogen bond network within the propellant, preventing or slowing the relatively low-energy proton transfer reaction between hydroxylammonium and nitrate, and thereby reducing the concentration of highly reactive nitric acid in the mixture. While the presence of water is beneficial for chemical mode, it is detrimental for electric electrospray mode. Water has a relatively high vapor pressure and is therefore volatile in vacuum environment. This leads to bubble formation in the electrospray feed system which prohibits or causes intermittent Taylor cone formation, adversely affecting ion and droplet extraction, and correspondingly affecting propulsion performance. Essentially, capillary electrospray of a high water content monopropellant is impossible. The HAN-[Emim][$EtSO_4$] propellant investigated here has very little to no water content. Recent nuclear magnetic resonance spectroscopy (HNMR) studies have shown that the synthesis path used in this work has <1% water content [12].

The chemical structure of the HAN-[Emim][$EtSO_4$] propellant constituents is shown in Figure 2. The chemical formula for $[Emim]^+$ $[EtSO_4]^-$ is $[C_6H_{11}N_2]^+$ $[C_2H_5SO_4]^-$. An important point is that HAN has two stable configurations, an ionic and covalent arrangement [66], and both of these are shown in Figure 2. In gas phase, there are three stable forms of HAN as a single molecule (monomer). All three are hydrogen bonded and do not show proton transfer from nitric acid to hydroxylamine (all three are referred to as covalent form). In this covalent form, the HAN molecule chemical formula is [$HONH_2$][HNO_3] (note: [$HONH_2$] will be referred to as [HA-H]) with multiple hydrogen bonds between the hydroxylamine and nitric acid molecules. However, a HAN cluster ([HAN]$_2$ dimer) can have an ionic form where the nitric acid proton has been transferred to the hydroxylamine resulting in hydroxylammonium and nitrate [66]. In this case, the HAN molecule chemical formula is $[HONH_3]^+$ $[NO_3]^-$ (note: $[HONH_3]^+$ will be referred to as $[HA]^+$) with an ionic bond between the molecules. The proton transfer reaction is relatively low energy of 15 kcal/mol (0.65 eV/molecule), suggesting that it may be possible for both ionic and covalent forms to exist together in solution. In the liquid phase of the propellant under investigation here, the plentitude of this proton transfer reaction and the resulting concentrations of hydroxylamine/hydroxylammonium and nitric acid/nitrate are unknown. But both appear to be observed in the mass spectra presented below.

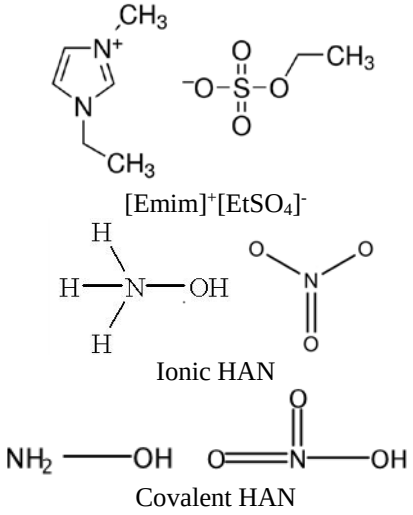

Figure 2: Chemical structure of the constituents of the HAN-based monopropellant. $[Emim]^+$ $[EtSO_4]^-$ and both the ionic $[HA]^+$ $[NO_3]^-$ and covalent [HA-H][HNO_3] forms of HAN.

Table 1 lists the theoretically calculated mass of species combinations that may be emitted via electrospray based on the possible constituents within the propellant. The masses calculated are for both ionic and covalent HAN, for solvated states up to n = 2. These tables are for both anion and cation emission modes, and are all singly-

charged species. The gray highlighted cells have a covalent constituent of HAN. A complete HAN molecule can be either the covalent or ionic form as there is no difference in the mass. Electrospray emission of ion masses within the range of these species (0-600 amu) is the focus of this work.

Table 1: Theoretical mass of possible species combinations based on the constituents within the HAN-[Emim][$EtSO_4$] propellant mixture.

Anion Emission Ion Combinations			Cation Emission Ion Combinations		
Specie	**Mass (amu)**	**n**	**Specie**	**Mass (amu)**	**n**
[NO3]-	62	0	[HA]+	34	0
[EtSO4]-	126.1	0	[Emim]+	111.2	0
[HA-H] [NO3]-	95	1	[HA-H] [HA]+	67	1
[HNO3] [NO3]-	125	1	[HNO3] [HA]+	97	1
[HAN] [NO3]-	158	1	[HAN] [HA]+	130	1
[HA-H] [EtSO4]-	159.1	1	[HA-H] [Emim]+	144.2	1
[HNO3] [EtSO4]-	189.1	1	[HNO3] [Emim]+	174.2	1
[HAN] [EtSO4]-	222.1	1	2[HA]+ [EtSO4]-	194.1	1
[Emim]+ 2[NO3]-	235.2	1	[HAN] [EMIM]+	207.2	1
[HA]+ 2[EtSO4]-	286.2	1	[HA]+ [EMIM]+ [EtSO4]-	271.3	1
[Emim]+ [NO3]- [EtSO4]-	299.3	1	2[Emim]+ [NO3]-	284.4	1
[Emim]+ 2[EtSO4]-	363.4	1	2[Emim]+ [EtSO4]-	348.5	1
2[HA-H] [NO3]-	128	2	2[HA-H] [HA]+	100	2
2[HNO3] [NO3]-	188	2	2[HNO3] [HA]+	160	2
[HA-H] [HAN] [NO3]-	191	2	[HA-H] [HAN] [HA]+	163	2
2[HA-H] [EtSO4]-	192.1	2	2[HA-H] [Emim]+	177.2	2
[HNO3] [HAN] [NO3]-	221	2	[HNO3] [HAN] [HA]+	193	2
2[HNO3] [EtSO4]-	252.1	2	2[HAN] [HA]+	226	2
2[HAN] [NO3]-	254	2	[HA-H] 2[HA]+ [EtSO4]-	227.1	2
[HA-H] [HAN] [EtSO4]-	255.1	2	2[HNO3] [Emim]+	237.2	2
[HA-H] [Emim]+ 2[NO3]-	268.2	2	[HA-H] [HAN] [EMIM]+	240.2	2
[HNO3] [HAN] [EtSO4]-	285.1	2	[HNO3] 2[HA]+ [EtSO4]-	257.1	2
[HNO3] [Emim]+ 2[NO3]-	298.2	2	[HNO3] [HAN] [EMIM]+	270.2	2
2[HAN] [EtSO4]-	318.1	2	[HAN] 2[HA]+ [EtSO4]-	290.1	2
[HA-H] [HA]+ 2[EtSO4]-	319.2	2	2[HAN] [Emim]+	303.2	2
[HAN] [Emim]+ 2[NO3]-	331.2	2	[HA-H] [HA]+ [EMIM]+ [EtSO4]-	304.3	2
[HA-H] [Emim]+ [NO3]- [EtSO4]-	332.3	2	[HA-H] 2[Emim]+ [NO3]-	317.4	2
[HNO3] [HA]+ 2[EtSO4]-	349.2	2	[HNO3] [HA]+ [EMIM]+ [EtSO4]-	334.3	2
[HNO3] [Emim]+ [NO3]- [EtSO4]-	362.3	2	[HNO3] 2[Emim]+ [NO3]-	347.4	2
[HA]+ [HAN] 2[EtSO4]-	382.2	2	3[HA]+ 2[EtSO4]-	354.2	2
[HAN] [Emim]+ [NO3]- [EtSO4]-	395.3	2	[HAN] [HA]+ [Emim]+ [EtSO4]-	367.3	2
[HA-H] [Emim]+ 2[EtSO4]-	396.4	2	[HAN] 2[Emim]+ [NO3]-	380.4	2
2[Emim]+ 3[NO3]-	408.4	2	[HA-H] 2[Emim]+ [EtSO4]-	381.5	2
[HNO3] [Emim]+ 2[EtSO4]-	426.4	2	[HNO3] 2[Emim]+ [EtSO4]-	411.5	2
2[HA]+ 3[EtSO4]-	446.3	2	2[HA]+ [Emim]+ 2[EtSO4]-	431.4	2
[HAN] [Emim]+ 2[EtSO4]-	459.4	2	[HAN] 2[Emim]+ [EtSO4]-	444.5	2
2[Emim]+ 2[NO3]- [EtSO4]-	472.5	2	3[Emim]+ 2[NO3]-	457.6	2
[HA]+ [Emim]+ 3[EtSO4]-	523.5	2	[HA]+ 2[Emim]+ 2[EtSO4]-	508.6	2
2[Emim]+ [NO3]- 2[EtSO4]-	536.6	2	3[Emim]+ [EtSO4]- [NO3]-	521.7	2
2[Emim]+ 3[EtSO4]-	600.7	2	3[Emim]+ 2[EtSO4]-	585.8	2

B. Electrospray Source

The electrospray source has been described in previous work [11, 54, 55, 67]. A photograph of the electrospray source is shown in Figure 3A. The source has an extractor plate with a 1.5-mm-diameter aperture and a conductive 50-µm ID stainless steel capillary needle (PicoTip MT320-50-5-5) emitter. The emitter tip and extractor are set approximately 1.5 mm apart, yielding an approximate pass through angle of 30° off axis emission. The emitter-extractor assembly is mounted on a rotatable stage. The emitter-extractor assembly and rotation stage are mounted at the end of an arm attached to a vacuum flange with propellant/liquid feed-through and high-voltage feed-through connections. This entire assembly, shown in Figure 3B, is secured to a vacuum chamber and operated in vacuum at a nominal $1x10^{-6}$ Torr. A 100-µm ID silica capillary connects the emitter capillary to the propellant reservoir. The propellant reservoir is situated on a syringe pump (Harvard Elite Module Picopump) external to vacuum, thus requiring the silica capillary to pass through a custom feed-through on the vacuum flange.

For the experiments reported here, a 3.0 kV potential difference is applied between the emitter and extractor. When referenced to facility ground, the emitter is biased at +0.5 kV and the extractor at -2.5 kV for cation emission. Anion emissions are obtained by switching the polarity, i.e. emitter bias of -0.5 kV and the extractor at +2.5 kV. This potential difference has been shown to provide stable emission of this liquid for the capillary size used here [11], and agrees well with theoretical predictions of the starting voltage for electrosprayed liquids and liquid metal ion sources [68]. Flow rates investigated in this study cover the range of 2.0 pL/s to 3.0 nL/s, with corresponding emitter currents of 600 to 1100 nA. For most flow rates spectra were acquired at emitter angular orientations of -30º to 10º in 5º increments, and at -45°.

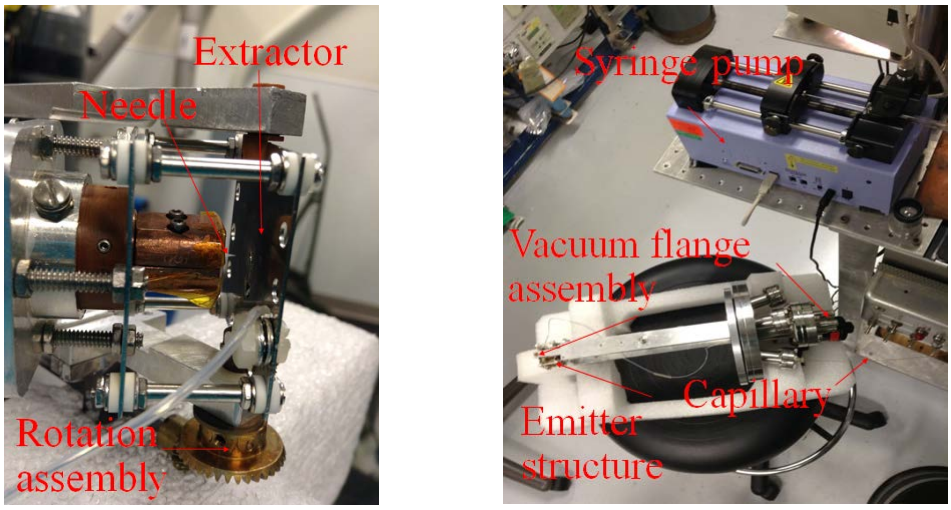

Figure 3: Photograph of (A) zoomed in view showing emitter and extractor mounted on rotation stage and (B) emitter structure mounted to vacuum flange outside the vacuum chamber showing capillary feed tube and syringe propellant pump.

C. Quadrupole Mass Spectrometer

The diagnostic used in this study is a quadrupole mass spectrometer. A schematic of the general setup is shown in Figure 4 and the Extrel quadrupole used here has been described previously [51, 69-71]. The faraday cup, QCM, and RPA are not used for data collection in this study. The emitted electrospray species initially pass through a series of ion lenses to focus the ion beam before it enters the quadrupole. The charged particles then pass through the quadrupole where the mass-to-charge ratio (m/q) of the particles selected for passage. Next the selectively filtered particle beam passes through the RPA. In these experiments the RPA has not been biased to ensure particles of all energies at the investigated m/q value can pass through. Finally, the particles are detected using an off-axis channeltron single-channel electron multiplier with an accompanying deflector. The channeltron is connected to an event counter such that the arrival of a particle at the channeltron registers an event or "count". At a particular m/q, the counts are integrated for three 25 ms durations for cation mode and three 100 ms durations for anion mode. A longer integration time is used in anion mode to average out the larger noise inherent to anion mode.

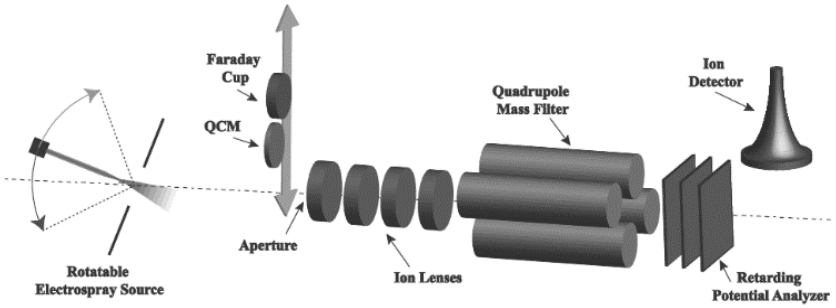

Figure 4: Schematic of the quadrupole mass spectrometry system used here, and is the same as described by Miller et al. [51].

III. Results

Experimental mass spectrum results were obtained for cation and anion emission modes of the electrospray source operating with the HAN-[Emim][$EtSO_4$] monopropellant. Flow rates of 2.0 pL/s to 3.0 nL/s and angular orientations of -30º to 10º in 5º increments and -45° were investigated. All mass spectrum data are presented as relative counts. For anion mode, the absolute number of counts measured across all angles and flow rates have been divided by the number of counts corresponding to the [$EtSO_4$] anion at -15º and 5 pL/s flow rate of 9.638×10^4. In cation mode, the absolute number of counts measured across all angles and flow rates have been divided by the number of counts corresponding to the [Emim] cation at -15° and 5 pL/s flow rate, which had a counts value of 1.478×10^4. The results presented below are divided into sections that focus on the anion and cation modes, respectively. The goal is to compare observed peaks in the mass spectra with anticipated or expected ion masses based on theoretical combinations of the four constituent ions, masses given in Table 1.

Analysis of flow rate and angular orientation effects showed trends typical of what is found in literature, and therefore will only be briefly discussed here. As the emitted ions pass through the quadrupole at significant kinetic energy, the resolution of the spectra peaks tends to be poorer, the "zero mass" tends to extend to larger *m/q* ratios, and a general overall baseline is present in the spectrum. These results are similar to phase space literature data over *m/q*, angle, and intensity [51, 69]. A larger droplet concentration, identified as an overall baseline in the spectrum, was observed on centerline and increased with flow rate. The presence of droplets extended to approximately 15° off-axis, a result that is well-described in the literature [50, 51, 72]. No emitted species were found at an angle of -45°. Spectra were symmetric about centerline, and in some cases included dual peaks at 5° to 10° off-axis due to emission from the neck region of the Taylor cone, a result previously identified by Lozano [73]. As flow rate increased the intensity of peaks in the spectra decreased, signifying a decrease in ion emission and increase in droplet emission, another result that is well-described in the literature [50, 51, 69, 74, 75].

A. Anion Mode

Data collected for a 0-900 *m/q* range are shown in Figure 5 for selected flow rates at angular orientation of -15º. Peaks in the mass spectrum are observed on top of a significant background profile, complicating the assignment of their respective intensities, particularly at values below 150 *m/q*. Peaks are observed out to about 300 *m/q* while the background persists to about 700 *m/q* at all flow rates shown. A peak at 278 *m/q* has the most significant signal-to-noise ratio with respect to the baseline. The mass spectra appear similar over the two orders of volumetric flow rate magnitude examined, with only slight increases in the relative baseline as flow rate is increased. The dearth of peaks in the spectra at mass values above 300 *m/q* indicate that higher order solvated states (such as the $n > 2$ clusters) are not present at significant levels. With the absence of apparent species above 300 *m/q*, the quadrupole was operated to interrogate the 5-500 *m/q* range.

Example mass spectra for anion mode emission from 20 to 300 *m/q* is shown in Figure 6 for flow rates 5 pL/s and 500 pL/s at an angular orientation of -15º and -15°, respectively. Data are not reported at *m/q* less than 20 *m/q* due to the low quadrupole mass offset (zero mass). The droplet baseline signal has been removed shifting the spectrum down. From this point, any presented spectrum has had the baseline removed for clarity.

Figure 6 shows clear peaks in the mass spectrum for anion emission of the HAN-[Emim][$EtSO_4$] monopropellant. In this spectra, peaks are evident at 44, 60, 78, 96, 124, 146, 188, 194, 210, 220, 235, 250, and 278 *m/q*. Over all flow rates and angular orientations investigated, these are the dominant peaks found in all spectra. The two monomer anion constituents of the propellant, as identified in Table 1, appear to be present in the spectra. The [$EtSO_4$] anion (mass

126 amu) is at 124 *m/q* and the nitrate [NO_3] anion (mass 62 amu) is at 60 *m/q*. The 124 *m/q* peak may also contain the [HNO_3][NO_3]$^-$ pairing which has a mass of 125 amu. The 62 *m/q* peak has an intensity that is 16.7% larger than the 124 *m/q* peak at 5 pL/s. At 500 pL/s the 124 *m/q* peak intensity has dropped to 68% of what it was at 5 pL/s, and now the 60 *m/q* peak intensity is less than the 124 *m/q*. Specifically the 60 *m/q* intensity has decreased 60% from 1.17 to 0.45 between the 5 to 500 pL/s flow rates.

Also in Figure 6, the peaks at 94, 188, 194, 220, 235, and 250 *m/q* appear to correspond with some of the expected n = 1 and n = 2 solvated states of Table 1. The peak at 94 *m/q* may be a hydroxylamine [HA-H] paired with nitrate [NO3]$^-$, which has a mass of 95 amu. A combination of 2[HNO_3] with [NO_3]$^-$ has a mass of 188 amu and corresponds with the 188 *m/q* peak. This 188 *m/q* peak may also be [HNO_3] [$EtSO_4$]$^-$ (mass 189 amu), which would indicate swapping of bonded species within the liquid. In other words, this emitted ion is a combination of a neutral covalent HAN species bonded with the [Emim][$EtSO_4$] anion. The 192 *m/q* peak may be due to the presence of [HA-H] [HAN] [NO_3]$^-$ (mass 191 amu), and would indicate a pairing of a complete HAN molecule with hydroxylamine and nitrate species within the same emitted ion. The combination of 2[HA-H] [$EtSO_4$]$^-$ (mass 192 amu) may also be present within the 192 *m/q* peak. The peak at 220 *m/q* may be due to the combination of [HNO_3] [HAN] [NO_3]$^-$ (mass 221 amu), and would also indicate there is pairing of HAN molecule with nitric acid and nitrate. This peak could also be due to [HAN] [$EtSO_4$]- (mass 222 amu), which would indicate pairing of anions from both HAN and [Emim][$EtSO_4$] within the same emitted species. The peak at 235 *m/q* appears to correspond with [Emim]$^+$ 2[NO_3]$^-$ (mass 235 amu), where [Emim] is now bonded with the nitrate from the ionic form of HAN. The peak at 250 *m/q* appears to correspond with 2[HNO_3] [$EtSO_4$]$^-$ (mass 252 amu). Table 2 summarizes these observed peaks in the mass spectra and their correlated species.

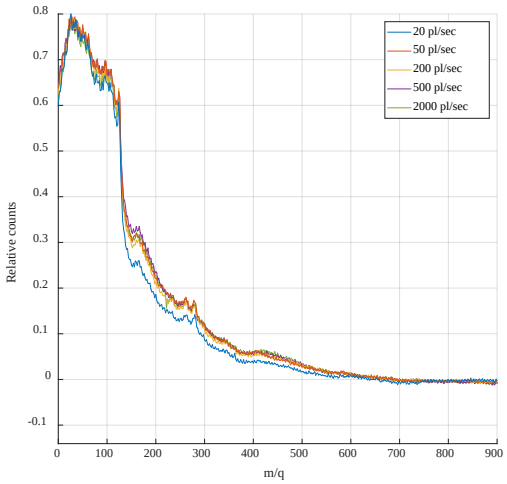

Figure 5: Anion mass spectra out to 1000 *m/q* for different flow rates at -15° angular orientation.

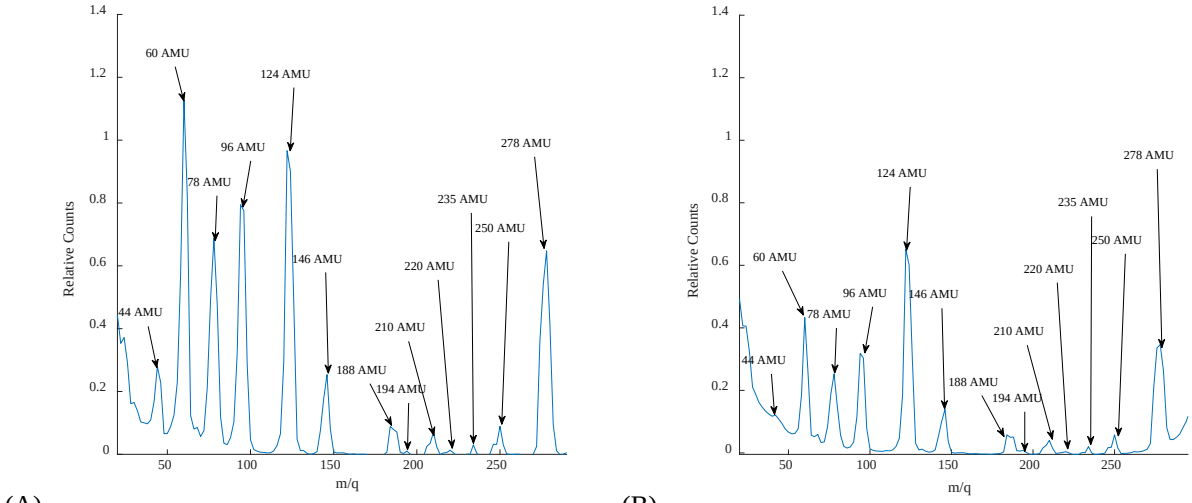

(A) (B)

Figure 6: Example anion mass spectrum at (A) 5 pL/s and (B) 500 pL/s at -15° off axis.

Figure 6 also shows peaks in the spectra that do not directly correlate with the theoretical mass calculations in Table 1. These are the peaks at 44, 78, 146, 210, and 278 *m/q*. Some of these peaks are believed to be due to ion fragmentation. These peaks will be discussed in the discussion section below.

B. Cation Mode

Extended mass spectra were acquired for different flow rates in cation mode at -15° off axis, and are plotted for a range of 0-500 *m/q* in Figure 7. The y-axis has been normalized as described above to the $[Emim]^+$ cation value. The only discernable peak above 200 *m/q* appears at 344 *m/q*; however, even this peak is dwarfed by the single $[Emim]^+$ ion emission (111 *m/*q) whose signal is ~50 times larger. This small peak may be a dimer (n = 1) corresponding to $2[Emim]^+$ $[EtSO_4]^-$ (mass of 348 amu) or it may be the trimer (n = 2) $[HNO_3]$ $2[Emim]^+$ $[NO_3]^-$ (mass of 347 amu). The spectra do not show any other peaks beyond 200 *m/q*. Therefore the range 20 to 200 *m/q* is further investigated.

A representative cation mass spectrum from 20 to 200 *m/q* can be seen below in Figure 8. Figure 8 shows clear peaks at 28, 40, 54, 68, 82, 94, 110, and 138 *m/q*. Over all flow rates and angular orientations investigated these are the only clear peaks within this mass range. The two monomer cations may be present at 28 and 110 *m/q*. The 110 *m/q* peak likely corresponds with $[Emim]^+$ (mass 111 amu). But $[HA]^+$ cation has a mass of 34 amu, which is 6 amu above the 28 amu of the peak. The peak at 110 *m/q* in Figure 8 (5 pL/s at -15°) has a value of 1 denoting the normalization case, and the peak at 28 *m/q* is 43% of the 110 *m/q* peak. At 500 pL/s the peak at 110 *m/q* has decreased to 69% of its 5 pL/s value, and the peak at 28 m/q has decreased by 27% in magnitude.

Table 2: Comparison of measured (Figure 6) and theoretical mass (Table 1) of identified anion species.

Measured *m/q (amu)*	Assigned Species	Theoretical *m/q (amu)*
60	$[NO_3]^-$	62
96	[HA-H] [NO3]-	95
124	[HNO3] [NO3]- And/Or [EtSO4]-	125, 126
188	2[HNO3] [NO3]- And/Or [HNO3] [EtSO4]-	188, 189
194	[HA-H] [HAN] [NO3]- And/Or 2[HA-H] [EtSO4]-	191, 192
220	[HNO3] [HAN] [NO3]- And/Or [HAN] [EtSO4]-	221, 222
235	[Emim]+ 2[NO3]-	235
250	2[HNO3] [EtSO4]-	252

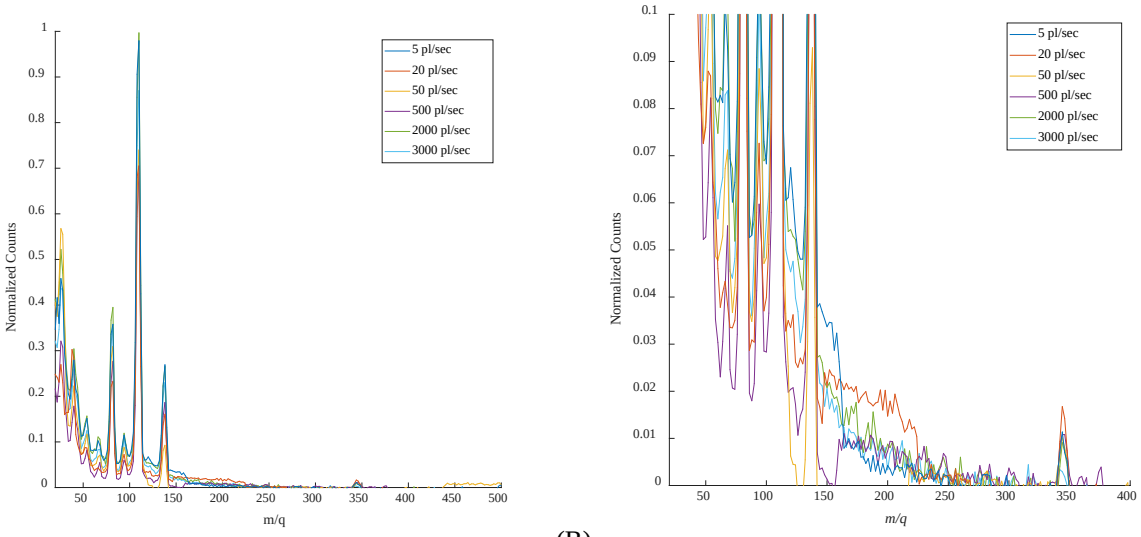

Figure 7: Cation mass spectra at -15° off axis over multiple flow rates (A) normal view and (B) zoomed in.

There are several peaks that can be related to dimers and trimers in Figure 8. Notably, the peaks at 68 and 94 *m/q*. The peak at 94 *m/q* may correspond to $[HNO_3]$ $[HA]^+$ (mass 97 amu), which would indicate bonding of covalent and ionic HAN species. The peak at 68 *m/q* may be [HA-H] $[HA]^+$ (mass 67 amu), which again would indicate covalent and ionic HAN species bonding. A summary of these observed mass spectra peaks and their corresponding species based on comparison with theoretical mass calculation is given in Table 3. The rest of the peaks at 40, 54, 82, and 138 *m/q* may be associated with fragmentation of the ions, and this will be discussed further in the discussion section below.

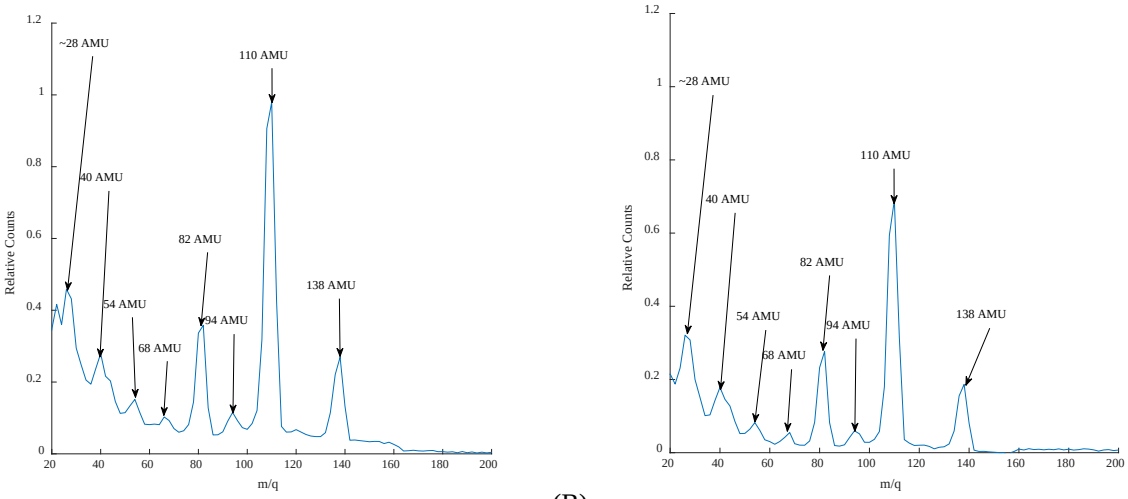

Figure 8: Cation mass spectrum at (A) 5 pL/s and (B) 500 pL/s flow-rate at -15° off axis.

IV. Discussion

A. Monomer Species are Present in the Spectra

There are four possible monomer species for the HAN-[Emim][$EtSO_4$] liquid: cations: $[Emim]^+$ (111 amu), $[HA]^+$ (34 amu), and anions: $[NO_3]^-$ (62 amu), $[EtSO_4]^-$ (126 amu). The $[Emim]^+$ and $[NO_3]^-$ are present in the spectra. Figure 8 shows a peak at 110 amu corresponding with $[Emim]^+$, and, as Table 1 shows, there are no other identified species combinations that are expected to give rise to that mass. Figure 6 clearly shows a peak at 60 amu corresponding with $[NO_3]^-$, and there are no other identified species combinations that are expected to give rise to that mass. The $[EtSO_4]^-$ anion may also be present because a peak is evident at 124 amu in Figure 6, however, this peak may also contain $[HNO_3][NO_3]^-$ which has a mass of 125 amu, and will be discussed below. It is unclear what fraction of the intensity of the 124 amu mass spectrum peak corresponds to $[EtSO_4]^-$ vs. $[HNO_3][NO_3]^-$, both have been observed in the literature [76, 77]. Of the four monomers identified, the presence of $[HA]^+$ cation is the most questionable. There is no identified peak at its mass of 34 amu in any of the spectra. The closest peak is at 28 amu as shown in Figure 8. The mass resolution of the quadrupole instrument was set at 2 amu. An experiment conducted directly before these data with a different non-DSIL ionic liquid showed agreement with expected species to within 2 amu. So we expect the *m/q* of peaks in the spectra to be accurate to within 2-3 amu. Therefore at this time the $[HA]^+$ cation cannot be definitively assigned within the spectra.

Table 3: Comparison of measured (Figure 8) and theoretical mass (Table 1) of identified cation species.

Measured *m/q (amu)*	**Assigned Species**	**Theoretical *m/q (amu)***
28	[HA]+	34
68	[HA-H] [HA]+	67
94	[HNO3] [HA]+	97
110	[Emim]+	111
344	[HNO3] 2[Emim]+ [NO3]- And/or 2[Emim]+ [EtSO4]-	347, 348

B. Presence of Proton-Transfer Species

Proton-transfer species are present in both the cation and anion spectra. The proton-transfer species of HAN ($[HA]^+[NO_3]^-$, the ionic form of HAN) are [HA-H][HNO_3], and these are also referred to as the covalent form of HAN. Numerous peaks in the anion and cation spectra may contain these species, for instance 124 and 188 amu in the anion spectra of Figure 6. It is not unusual to see such proton-transfer species in the presence of liquids with a nitrate functional group. Prince et al. investigated neat IL 2-hydroxylethylhydrazinium nitrate ($[HEH]^+[NO_3]^-$, a.k.a. HEHN) [76]. Proton transfer between these species results in [HE][HNO_3], and they saw both of these species in the mass spectra. They used an externally wetted titanium emitter and observed $[HE][HEH]^+$ and $[HNO_3][NO_3]^-$ dimers along with $2[HNO_3][NO_3]^-$ trimer. Interestingly they did not identify $[HNO_3][HEH]^+$ or $[HE][NO_3]^-$, suggesting the proton-transferred species only pair with their counterpart. Our results show both covalent species paired with the monomer

anion and cation. Specifically the anion spectra of Figure 6 show $[HNO_3][NO_3]^-$ and [HA-H]$[NO_3]^-$ at 94 and 124 amu, respectively. Our cation spectra of Figure 8 show [HA-H]$[HA]^+$ and $[HNO_3][HA]^+$ at 68 and 94 amu, respectively. Similar to Prince et al. [76] we also identify $2[HNO_3][NO_3]^-$ at 188 amu in our spectra of Figure 6. They also identified additional solvated states of $[HE][HEHN]_n[HEH]^+$, but no solvated states of $[HNO_3][HEHN]_n[HEH]^+$. We do not observe any cation solvated states with a full [HAN] molecule. However, we do see anion solvated states with both [HA-H] and $[HNO_3]$, but only for n = 1. Specifically we identify [HA-H][HAN]$[NO_3]^-$ and $[HNO_3][HAN][NO_3]^-$ at 194 and 220 amu, respectively, in Figure 6. Finally we also see proton-transfer species pairing with cations and anions of the solvent. In particular [HNO3]$[EtSO_4]^-$, 2[HA-H]$[EtSO_4]^-$, and 2[HNO3]$[EtSO_4]^-$ anions in Figure 6 and $[HNO_3]2[Emim]^+[NO_3]^-$ cation of Figure 8.

The results presented here indicate proton-transferred species can be emitted from a different molecule with nitrate functional group, HAN as opposed to HEHN. Further, the results presented here indicate that these species can be emitted from a mixture, which has never before been demonstrated. Our results indicate that both proton-transferred covalent species can be paired with both ionic species for HAN in mixture with [Emim][$EtSO_4$], unlike the neat IL results for HEHN. Also, results presented here show these species are present over a wider range of flow rates than previously thought, from the low flow rate externally wetted studies of Prince et al. (~2 ng/s) [76], to the higher flow rates investigated here (7 – 4600 ng/s).

C. Swapping of Anions and Cations in the Mixture

Numerous species identified in the spectra show pairing of ionic and covalent forms of HAN, as well as swapping of cations and anions between the constituents of the mixture. Swapping of anions and cations is possible because the IL investigated here is a mixture. . Here, we find in the electrospray plume that [HAN] anion can bind with [Emim][$EtSO_4$] cation, and vice-versa. This type of behavior is also indicative that the mixture is a DSIL as opposed to a simple mixture [40].

Anion results of Figure 6 (Table 2) may indicate pairing of each $[HNO_3]$, $2[HNO_3]$, 2[HA-H], and [HAN] with $[EtSO_4]^-$. But interestingly, while we see 2[HA-H], we do not see [HA-H] paired with $[EtSO_4]^-$, which would appear at 160 amu. Also, while we see [HAN]$[EtSO_4]^-$ we do not see [HAN]$[NO_3]^-$. We identify $[Emim]^+$ paired with $2[NO_3]^-$, but the anion spectra do not show $[Emim]^+$ paired with $[EtSO_4]^-$. That is, the anion spectra do not show an [Emim][$EtSO_4$] combination. Of all possible dimer (n = 1) combinations identified in Table 1, we see half of them in the spectra. We do not see any species at 160 amu ([HAN]$[NO_3]^-$ or [HA-H]$[EtSO_4]^-$), nor do we see any species greater than 280 amu ($[HA]^+2[EtSO_4]^-$ or $[Emim]^+[EtSO_4]^-[NO_3]^-$ or $[Emim]^+2[EtSO_4]^-$). We do see a peak at 278 amu, but cannot link it directly to any of these species.

The absence of [Emim][$EtSO_4$] in the anion spectra may not be surprising considering the mole fraction of the mixture. While the mass fraction is 59% HAN to 41% [Emim][$EtSO_4$], the mole fraction is 78% HAN to 22% [Emim][$EtSO_4$], indicating there are 3.55 times as many HAN molecules as [Emim][$EtSO_4$] molecules. Based on this, one might expect more HAN-related species to be emitted into the plume. Considering only the monomers, Figure 6 for 5 pL/s does indicate $[NO_3]^-$ intensity at 60 amu is 17% higher than $[EtSO_4]^-$ intensity at 124 amu. However, this trend flips for the 500 pL/s case. Further, the contribution of $[EtSO_4]^-$ to the intensity at 124 amu is convoluted by the likely presence of $[HNO_3][NO_3]^-$. The spectra also show that numerous other species besides monomers are present in the plume (including droplets), and in some cases contain both HAN and [Emim][$EtSO_4$] related species. Unfortunately it is impossible using the current data to quantify the plume ratio of HAN-related vs [Emim][$EtSO_4$]-related species.

Numerous species were identified in the anion spectra showing swapping of anions and cations, but only one such specie has been identified within the cation spectra of Figure 8 (Table 3). Specifically the peak at 344 amu may be partially due to $[HNO_3]2[Emim]^+[NO_3]^-$, which has [Emim] cations paired with ionic and covalent forms of HAN. Interestingly this peak may also be due to $2[Emim]^+[EtSO_4]^-$, which would indicate that [Emim][$EtSO_4$] is present within the cation spectra. While we see $2[Emim]^+[EtSO_4]^-$, we do not see $2[Emim]^+[NO_3]^-$. Unlike the anion case, only three of the possible ten dimers are identified in the cation spectra.

D. Speculation on Remaining Peaks

Numerous peaks in the experimental mass spectra cannot be assigned based on the constituent ion pairings listed in Table 1. Specifically for the anion spectra, peaks at 44, 78, 146, 210, and 278 amu are unidentified, while for the cation spectra, peaks at 40, 54, 82, and 138 amu are unidentified. These may be fragments and/or impurities in the liquid. Ions and solvated states are known to fragment. Courtney and Shea have developed a technique for correcting for fragmentation in propulsion performance calculations [78]. Miller and Lozano have quantified fragmentation rates for an externally wetted emitter with [Emim][BF_4] [79]. Prince et al. observed fragmentation of the cation HEH^+ along the interior N-C bond resulting in $N_2H_4^+$ and $C_2H_5O^+$ [76]. They also observed these charged fragments and

their neutral species pairing with covalent proton-transfer species, i.e., [HE] pairing with $[C_2H_5O]^+$. Similar phenomenon may be present in the plume of the HAN-[Emim][$EtSO_4$] propellant.

We speculate on possible fragmentation species and correlate their theoretical mass with anomalous peaks measured in the spectra. Specifically, referring to Figure 2, we assume [Emim] will fragment along the N-C bond, possibly resulting in a free methyl group (CH_3), ethyl group (C_2H_5), and imidazolium ring ($C_3H_3N_2$). We assume [$EtSO_4$] will fragment along the O-C and/or C-C bond, possibly resulting in a free methyl group (CH_3), ethyl group (C_2H_5), and sulfur tetroxide (SO_4). We assume no fragmentation of HAN species. With these assumed possibilities we calculate the theoretical mass of these fragments paired with other species expected within the liquid (e.g., [HA-H], [HNO_3], etc.). NIST was also used when identifying the [$EtSO_4$] data, as there is spectral data (including fragments) on diethyl sulfate, showing the constitutive elements/molecules it is likely to break into [80]. Results are given in Table 4.

Table 4: Speculation of possible fragments and/or impurities within the HAN-[Emim][$EtSO_4$] mass spectrum.

Species Type	Measured *m/q (amu)*	Possible Species	Theoretical *m/q (amu)*
Anion	44	?	
Anion	78	CH3 $[NO_3]^-$	77
Anion	146	2[HA-H] CH3 $[NO_3]^-$	143
Anion	210	Impurity in [Emim][$EtSO_4$]	
Anion	278	Impurity in [Emim][$EtSO_4$]	
Cation	40	?	
Cation	54	?	
Cation	82	2[HA-H]CH3	81
Cation	138	2[HNO3]CH3 And/or Impurity in [Emim][$EtSO_4$]	141

Peaks in the anion spectra at 78 and 146 amu may be due to combinations of nitrate with a methyl group and [HA-H]. The peak at 44 amu remains unidentified. We believe the peaks at 210 and 278 amu are due to an impurity (impurities?) within the [Emim][$EtSO_4$]. Our recent unpublished work has studied plume mass spectra of neat [Emim][$EtSO_4$], and this peak appears in the spectrum of neat [Emim][$EtSO_4$]. The [Emim][EtSO4] as purchased form Sigma Aldrich is $\geq$ 95% pure. We remove any volatile impurities by placing it in vacuum for extended duration; however, non-volatile impurities remain and these may be producing the peaks at 210 and 278 amu. Peaks in the cation spectra at 40 and 54 amu remain unidentified. Peaks at 82 and 138 amu may be combination of a methyl group with covalent HAN species. We also see the 138 amu peak in neat [Emim][$EtSO_4$] spectra, so this specie may also be an impurity.

V. Conclusion

The HAN-based monopropellant mixture HAN-[Emim][$EtSO_4$] electrosprays stably over a wide flow rate range of 2 pL/s to 3 nL/s in a 50 μm capillary emitter. The mass spectrum examined over this flow rate range contains small n = 0, 1, 2 solvated states in addition to droplets. The ion species mass spectra were investigated in detail over a mass range of 0 – 600 amu. The angular distribution of the plume mass spectra and the effects of flow rate agree with the existing literature. In that respect, the liquid is similar to other previously investigated electrospray propellants.

Plume mass spectra of the HAN-[Emim][$EtSO_4$] mixture showed results new and novel for electrospray propellants. First, both ionic and covalent forms of HAN were observed. While proton-transfer species have been observed previously, the results here show for the first time that both proton-transferred covalent species can be paired with both ionic species for HAN. Also, these covalent forms of HAN are observed to bond and be emitted with the anion of the solvent [Emim][$EtSO_4$]. But they do not appear to be as readily emitted with the cation. Evidence of proton-transfer species in electrospray plume has now been demonstrated over a much wider flow rate range (7-4600 ng/s). Second, because the liquid is a double-salt ionic liquid (i.e., a mixture), we observe swapping of anion and cation species between the constituents. This swapping is most evident in anion mode, where numerous forms of HAN ([HNO_3], 2[HNO_3], 2[HA-H], and [HAN]) appear in the spectra attached with $[EtSO_4]^-$. Only one such possible specie was identified in cation mode, $[HNO_3]2[Emim]^+[NO_3]^-$, but this may also be $2[Emim]^+[EtSO_4]^-$. While [Emim][EtSO4] neutral pair may be found in cation spectra, it is noticeably absent from the anion spectra. In fact, both cation and anion spectra appear to contain more HAN than [Emim][$EtSO_4$] related species. This may be expected since the mole fraction of HAN to [Emim][$EtSO_4$] is 3.55:1, but cannot be quantitatively evaluated with the existing data. Finally, numerous spectrum peaks remain unidentified, for both cation and anion modes. At least two, and maybe three, of these peaks is likely due to an impurity in the [Emim][$EtSO_4$] because the same peak appears in the

mass spectrum of neat [Emim][$EtSO_4$] without HAN. Other peaks may also be impurities or fragments. Emitted electrospray ions and droplets are known to fragment. Our speculation of possible fragmentation paths for [Emim][$EtSO_4$] may have identified four of the anomalous peaks, but still three remain. Future investigations should focus on conclusive identification of these species.

VI. Acknowledgments

Support for this work was provided through the NASA Marshall Space Flight Center, NASA grant NNM15AA09A, and the Air Force University Nanosatellite Program through the Utah State University Research Foundation, grant CP0039814. Additional support was provided by NASA Goddard Space Flight Center through the NASA Undergraduate Student Instrument Project grant NNX16AI85A, and the University of Missouri System Fast Track Program. M. Wainwright thanks the Department of Education, the AFRL Kirtland and his co-authors all of whom made this research possible. He would also like to thank Dr. Riggins, his parents, and the department secretaries for the support they provided both directly and indirectly on this research, their assistance played no small part over the timeframe of this research.

VII. References

[1] Berg, S. P. "DEVELOPMENT OF IONIC LIQUID MULTI-MODE SPACECRAFT MICROPROPULSION SYSTEMS," *Aerospace Engineering*. Vol. Doctoral, Missouri University of Science and Technology, Rolla, MO, 2015.

[2] Berg, S. P., and Rovey, J. L. "Ignition Evaluation of Monopropellant Blends of HAN and Imidazole-Based Ionic Liquid Fuels," *50th Aerospace Sciences Meeting*. Nashville, TN, 2012.

[3] Berg, S. P., and Rovey, J. L. "Dual-Mode Propellant Properties and Performance Analysis of Energetic Ionic Liquids," *50th Aerospace Sciences Meeting*. Nashville, TN, 2012.

[4] Berg, S. P., and Rovey, J. L. "Assessment of Imidazole-Based Ionic Liquids as Dual-mode Spacecraft Propellants," *Journal of Propulsion and Power* Vol. 29, No. 2, 2013, pp. 339-351.

[5] Berg, S. P., and Rovey, J. L. "Decomposition of Monopropellant Blends of Hydroxylammonium Nitrate and Imidazole-Based Ionic Liquid Fuels," *Journal of Propulsion and Power* Vol. 29, No. 1, 2013, pp. 125-135. doi: 10.2514/1.b34584

[6] Berg, S. P., and Rovey, J. L. "Assessment of Multi-Mode Spacecraft Micropropulsion Systems," *50th AIAA/ASME/SAE/ASEE Joint Propulsion Conference*. American Institute of Aeronautics and Astronautics, Cleveland, OH., 2014.

[7] Berg, S. P., and Rovey, J. L. "Decomposition of a Double Salt Ionic Liquid Monopropellant on Heated Metallic Surfaces," *52nd AIAA/SAE/ASEE Joint Propulsion Conference*. Salt Lake City, UT, 2016.

[8] Berg, S. P., and Rovey, J. L. "Design and Development of a Multi-Mode Monopropellant-Electrospray Micropropulsion System," *30th Annual AIAA/USU Conference on Small Satellites*. Logan, UT, 2016.

[9] Berg, S. P., and Rovey, J. L. "Assessment of Multi-Mode Spacecraft Micropropulsion Systems," *Journal of Spacecraft and Rockets* Vol. 54, No. 3, 2017, pp. 592-601.

[10] Berg, S. P., and Rovey, J. L. "Decomposition of Double Salt Ionic Liquid Monopropellant in a Microtube for Multi-Mode Micropropulsion Applications," *53rd AIAA/SAE/ASEE Joint Propulsion Conference*. Atlanta, GA, 2017.

[11] Berg, S. P., Rovey, J. L., Prince, B., Miller, S., and Bemish, R. "Electrospray of an Energetic Ionic Liquid Monopropellant for Multi-Mode Micropropulsion Applications," *51st AIAA/SAE/ASEE Joint Propulsion Conference*. American Institute of Aeronautics and Astronautics, Orlando, FL., 2015.

[12] Mundahl, A., Berg, S. P., Rovey, J. L., Huang, M., Woelk, K., Wagle, D. V., and Baker, G. "Characterization of a Novel Ionic Liquid Monopropellant for Multi-Mode Propulsion," *53rd AIAA/SAE/ASEE Joint Propulsion Conference*. Atlanta, GA, 2017.

[13] Donius, B. R., and Rovey, J. L. "Analysis and Prediction of Dual-Mode Chemical and Electric Ionic Liquid Propulsion Performance," *48th Aerospace Sciences Meeting*. AIAA, Orlando, FL, 2010.

[14] Donius, B. R., and Rovey, J. L. "Ionic Liquid Dual-mode Spacecraft Propulsion Assessment," *Journal of Spacecraft and Rockets* Vol. 48, No. 1, 2011.

[15] Mundahl, A. J., Berg, S. P., and Rovey, J. L. "Linear Burn Rate of Monopropellant for Multi-mode Micropropulsion," *AIAA Propulsion and Energy Forum, 54th Joint Propulsion Conference*. Cincinnati, OH., 2018.

[16] Mundahl, A. J., Berg, S. P., and Rovey, J. L. "Linear burn rates of monopropellants for multi-mode micropropulsion," *52nd AIAA/SAE/ASEE Joint Propulsion Conference, 2016*. 2016.
[17] Ulybyshev, Y. P. "Optimization of multi-mode rendezvous trajectories with constraints," *Cosmic Research* Vol. 46, No. 2, 2008, p. 133. doi: 10.1134/s0010952508020056
[18] Hass, J., and Holmes, M. "Multi-Mode Propulsion System for the Expansion of Small Satellite Capabilities." 2010.
[19] Donius, B. R., and Rovey, J. L. "Ionic Liquid Dual-Mode Spacecraft Propulsion Assessment," *Journal of Spacecraft and Rockets* Vol. 48, No. 1, 2011, pp. 110-123. doi: 10.2514/1.49959
[20] Berg, S. P., and Rovey, J. L. "Assessment of High-Power Electric Multi-Mode Spacecraft Propulsion Concepts," *33rd Internation Electric Propulsion Conference*. Washington, D.C., 2013.
[21] Berg, S. P., and Rovey, J. L. "Assessment of Multimode Spacecraft Micropropulsion Systems," *Journal of Spacecraft and Rockets* Vol. 54, No. 3, 2017, pp. 592-601. doi: 10.2514/1.A33649
[22] Kluever, C. A. "Spacecraft optimization with combined chemical-electric propulsion," *Journal of Spacecraft and Rockets* Vol. 32, No. 2, 1995, pp. 378-380. doi: 10.2514/3.26623
[23] Kluever, C. A. "Optimal Geostationary Orbit Transfers Using Onboard Chemical-Electric Propulsion," *Journal of Spacecraft and Rockets* Vol. 49, No. 6, 2012, pp. 1174-1182. doi: 10.2514/1.60042
[24] Oh, D. Y., Randolph, T., Kimbrel, S., and Martinez-Sanchez, M. "End-to-End Optimization of Chemical-Electric Orbit-Raising Missions," *Journal of Spacecraft and Rockets* Vol. 41, No. 5, 2004, pp. 831-839. doi: 10.2514/1.13096
[25] Oleson, S. R., Myers, R. M., Kluever, C. A., Riehl, J. P., and Curran, F. M. "Advanced Propulsion for Geostationary Orbit Insertion and North-South Station Keeping," *Journal of Spacecraft and Rockets* Vol. 34, No. 1, 1997, pp. 22-28. doi: 10.2514/2.3187
[26] Mailhe, L. M., and Heister, S. D. "Design of a Hybrid Chemical/Electric Propulsion Orbital Transfer Vehicle," *Journal of Spacecraft and Rockets* Vol. 39, No. 1, 2002, pp. 131-139. doi: 10.2514/2.3791
[27] Chiu, Y.-h., and Dressler, R. A. *Ionic Liquids for Space Propulsion*. Washington, D. C.: ACS Publications, 2007.
[28] Gamero-Castaño, M. "Characterization of a Six-Emitter Colloid Thruster Using a Torsional Balance," *Journal of Propulsion and Power* Vol. 20, No. 4, 2004, pp. 736-741. doi: 10.2514/1.2470
[29] Mento, C. A., Sung, C.-J., Ibarreta, A. F., and Schneider, S. J. "Catalyzed Ignition of Using Methane/Hydrogen Fuel in a Microtube for Microthruster Applications," *Journal of Propulsion and Power* Vol. 25, No. 6, 2009, pp. 1203-1210. doi: 10.2514/6.2006-4871
[30] Chao, Y.-C., Chen, G.-B., Hsu, C.-J., Leu, T.-S., Wu, C.-Y., and Cheng, T.-S. "Operational characteristics of catalytic combustion in a platinum microtube," *Combustion science and technology* Vol. 176, No. 10, 2004, pp. 1755-1777. doi: 10.1080/00102200490487599
[31] Chen, C.-P., Chao, Y.-C., Wu, C.-Y., Lee, J.-C., and Chen, G.-B. "Development of a catalytic hydrogen micro-propulsion system," *Combustion science and technology* Vol. 178, No. 10-11, 2006, pp. 2039-2060. doi: 10.1080/00102200600793395
[32] Volchko, S. J., Sung, C.-J., Huang, Y., and Schneider, S. J. "Catalytic Combustion of Rich Methane/Oxygen Mixtures for Micropropulsion Applications," *Journal of propulsion and power* Vol. 22, No. 3, 2006, pp. 684-693. doi: 10.2514/1.19809
[33] Legge, R. S., and Lozano, P. "Electrospray Propulsion Based on Emitters Microfabricated in Porous Metals," *Journal of Propulsion and Power* Vol. 27, No. 2, 2011, pp. 485-495.
[34] Coffman, C. S., and Lozano, P. C. "On the Manufacturing and Emission Characteristics of Dielectric Electrospray Sources," *49th AIAA/ASME/SAE/ASEE Joint Propulsion Conference*. American Institute of Aeronautics and Astronautics, San Jose, CA., 2013.
[35] Mento, C. A., Sung, C.-J., Ibarreta, A. F., and Schneider, S. J. "Catalyzed Ignition of Methane/Hydrogen Fuel in a Microtube for Microthruster Applications," *Journal of Propulsion and Power* Vol. 25, No. 6, 2009, pp. 1203-1210. doi: 10.2514/1.42592
[36] Deans, M., and Schneider, S. "Development and Testing of a Methane/Oxygen Catalytic Microtube Ignition System for Rocket Propulsion," *48th AIAA/ASME/SAE/ASEE Joint Propulsion Conference & Exhibit*. American Institute of Aeronautics and Astronautics, Atlanta, GA, 2012.
[37] Mento, C., Sung, C.-J., Ibarreta, A., and Schneider, S. "Catalytic Ignition of Methane/Hydrogen/Oxygen Mixtures for Microthruster Applications," *42nd AIAA/ASME/SAE/ASEE Joint Propulsion Conference & Exhibit*. American Institute of Aeronautics and Astronautics, Sacramento, CA, 2006.
[38] Mundahl, A. J., Berg, S. P., and Rovey, J. L. "Linear Burn Rates of Monopropellants for Multi-Mode Micropropulsion," *52nd Joint Propulsion Conference*. Salt Lake City, UT, 2016.

[39] Cronin, J. T., and Brill, T. B. "Thermal decomposition of energetic materials. 8. Evidence of an oscillating process during the high-rate thermolysis of hydroxylammonium nitrate, and comments on the interionic interactions," *The Journal of Physical Chemistry* Vol. 90, No. 1, 1986, pp. 178-181. doi: 10.1021/j100273a040

[40] Chatel, G., Pereira, J. F. B., Debbeti, V., Wang, H., and Rogers, R. D. "Mixing ionic liquids-"simple mixtures" or "double salts"?," *Green Chemistry* Vol. 16, No. 4, 2014, pp. 2051-2083. doi: 10.1039/c3gc41389f

[41] Kirchner, B., Malberg, F., Firaha, D. S., and Hollóczki, O. "Ion pairing in ionic liquids," *Journal of Physics Condensed Matter* Vol. 27, No. 46, 2015. doi: 10.1088/0953-8984/27/46/463002

[42] MacFarlane, D. R., Forsyth, M., Izgorodina, E. I., Abbott, A. P., Annat, G., and Fraser, K. "On the concept of ionicity in ionic liquids," *Physical Chemistry Chemical Physics* Vol. 11, No. 25, 2009, pp. 4962-4967. doi: 10.1039/b900201d

[43] Marsh, K. N., Boxall, J. A., and Lichtenthaler, R. "Room temperature ionic liquids and their mixtures - A review," *Fluid Phase Equilibria* Vol. 219, No. 1, 2004, pp. 93-98. doi: 10.1016/j.fluid.2004.02.003

[44] Niedermeyer, H., Hallett, J. P., Villar-Garcia, I. J., Hunt, P. A., and Welton, T. "Mixtures of ionic liquids," *Chemical Society Reviews* Vol. 41, No. 23, 2012, pp. 7780-7802. doi: 10.1039/c2cs35177c

[45] Pape, J., Vikse, K. L., Janusson, E., Taylor, N., and McIndoe, J. S. "Solvent effects on surface activity of aggregate ions in electrospray ionization," *International Journal of Mass Spectrometry* Vol. 373, 2014, pp. 66-71. doi: 10.1016/j.ijms.2014.09.009

[46] Tokuda, H., Hayamizu, K., Ishii, K., Susan, M. A. B. H., and Watanabe, M. "Physicochemical properties and structures of room temperature ionic liquids. 2. variation of alkyl chain length in imidazolium cation," *Journal of Physical Chemistry B* Vol. 109, No. 13, 2005, pp. 6103-6110. doi: 10.1021/jp044626d

[47] Tokuda, H., Tsuzuki, S., Susan, M. A. B. H., Hayamizu, K., and Watanabe, M. "How ionic are room-temperature ionic liquids? An indicator of the physicochemical properties," *Journal of Physical Chemistry B* Vol. 110, No. 39, 2006, pp. 19593-19600. doi: 10.1021/jp064159v

[48] Ueno, K., Tokuda, H., and Watanabe, M. "Ionicity in ionic liquids: Correlation with ionic structure and physicochemical properties," *Physical Chemistry Chemical Physics* Vol. 12, No. 8, 2010, pp. 1649-1658. doi: 10.1039/b921462n

[49] Zhou, Y., Chingin, K., Li, C., Yang, S., Xiao, S., Zhu, L., and Chen, H. "Extractive electrospray ionization mass spectrometry of ionic liquids," *Analytical Methods* Vol. 6, No. 18, 2014, pp. 7190-7194. doi: 10.1039/c4ay00835a

[50] Miller, S. W., Prince, B. D., Bemish, R. J., and Rovey, J. L. "Electrospray of 1-Butyl-3-Methylimidazolium Dicyanamide Under Variable Flow Rate Operations," *Journal of Propulsion and Power* Vol. 30, No. 6, 2014, pp. 1701-1710.

[51] Miller, S. W., Prince, B. D., Bemish, R. J., and Rovey, J. L. "Mass spectrometry of selected ionic liquids in capillary electrospray at nanoliter volumetric flow rates," *52nd AIAA/SAE/ASEE Joint Propulsion Conference, 2016*. 2016.

[52] Lozano, P. C. "Energy properties of an EMI-Im ionic liquid ion source," *Journal of Physics D: Applied Physics* Vol. 39, No. 1, 2006, p. 126.

[53] Miller, S., Prince, B., Bemish, R., and Rovey, J. L. "Electrospray of 1-Butyl-3-Methylimidazolium Dicyanamide Under Variable Flow Rate Operations," *Journal of Propulsion and Power*, 2014.

[54] Miller, S. W., Prince, B. D., Bemish, R. J., and Rovey, J. L. "Electrospray of 1-Butyl-3-Methylimidazolium Dicyanamide Under Variable Flow Rate Operations," *Journal of Propulsion and Power* Vol. 30, No. 6, 2014, pp. 1701-1710. doi: 10.2514/1.B35170

[55] Miller, S. W., Prince, B. D., Bemish, R. J., and Rovey, J. "Mass Spectrometry of Selected Ionic Liquids in Capillary Electrospray at Nanoliter Volumetric Flow Rates," *52nd AIAA/SAE/ASEE Joint Propulsion Conference*. American Institute of Aeronautics and Astronautics, Salt Lake City, UT, 2016.

[56] Garoz, D., and Mora, J. F. d. l. "Charge emissions from electrosprays in vacuum: Mixtures of formamide with methylammonium formate," *Journal of Applied Physics* Vol. 113, No. 6, 2013, p. 064901. doi: 10.1063/1.4790580

[57] Guerrero, I., Bocanegra, R., Higuera, F. J., and De La Mora, J. F. "Ion evaporation from Taylor cones of propylene carbonate mixed with ionic liquids," *Journal of Fluid Mechanics* Vol. 591, 2007, pp. 437-459. doi: 10.1017/S0022112007008348

[58] Garoz, D., Bueno, C., Larriba, C., Castro, S., Romero-Sanz, I., Mora, J. F. d. l., Yoshida, Y., and Saito, G. "Taylor cones of ionic liquids from capillary tubes as sources of pure ions: The role of surface tension and electrical conductivity," *Journal of Applied Physics* Vol. 102, No. 6, 2007, p. 064913.

doi: 10.1063/1.2783769
[59] Katsumi, T., Hori, K., Matsuda, R., and Inoue, T. "Combustion Wave Structure of Hydroxylammonium Nitrate Aqueous Solutions," *46th AIAA/ASME/SAE/ASEE Joint Propulsion Conference & Exhibit*. American Institute of Aeronautics and Astronautics, 2010.
[60] Amrousse, R., Katsumi, T., Azuma, N., and Hori, K. "Hydroxylammonium nitrate (HAN)-based green propellant as alternative energy resource for potential hydrazine substitution: From lab scale to pilot plant scale-up," *Combustion and Flame* Vol. 176, No. Supplement C, 2017, pp. 334-348. doi: 10.1016/j.combustflame.2016.11.011
[61] Katsumi, T., Inoue, T., Nakatsuka, J., Hasegawa, K., Kobayashi, K., Sawai, S., and Hori, K. "HAN-Based Green Propellant, Application, and its Combustion Mechanism," *Combustion, Explosion, and Shock Waves* Vol. 48, No. 5, 2012, pp. 536-543. doi: 10.1134/S001050821205005X
[62] Vosen, S. R. "The Burning Rate of Hydroxylammonium Nitrate-Based Liquid Propellants," *Symposium (International) on Combustion* Vol. 22, No. 1, 1989, pp. 1817-1825. doi: 10.1016/S0082-0784(89)80195-X
[63] Vosen, S. R. "Hydroxylammonium nitrate-based liquid propellant combustion-interpretation of strand burner data and the laminar burning velocity," *Combustion and Flame* Vol. 82, No. 3–4, 1990, pp. 376-388. doi: http://dx.doi.org/10.1016/0010-2180(90)90009-G
[64] Vosen, S. R. "Concentration and Pressure Effects on the Decomposition Rate of Aqueous Hydroxylammonium Nitrate Solutions," *Combustion Science and Technology* Vol. 68, No. 4-6, 1989, pp. 85-99.doi: 10.1080/00102208908924070
[65] Kondrikov, B. N., Annikov, V. É., Egorshev, V. Y., and De Luca, L. T. "Burning of Hydroxylammonium Nitrate," *Combustion, Explosion and Shock Waves* Vol. 36, No. 1, 2000, pp. 135-145. doi: 10.1007/BF02701522
[66] Alavi, S., and Thompson, D. L. "Hydrogen bonding and proton transfer in small hydroxylammonium nitrate clusters: A theoretical study," *The Journal of Chemical Physics* Vol. 119, No. 8, 2003, pp. 4274-4282. doi: 10.1063/1.1593011
[67] Miller, S., Prince, B., and Rovey, J. "Capillary Extraction of the Ionic Liquid [Bmim][DCA] for Variable Flow Rate Operations," *48th AIAA/ASME/SAE/ASEE Joint Propulsion Conference & Exhibit*. American Institute of Aeronautics and Astronautics, Atlanta, GA, 2012.
[68] Mair, G. L. R. "Theoretical determination of current-voltage curves for liquid metal ion sources," *Journal of Physics D: Applied Physics* Vol. 17, No. 11, 1984, p. 2323.
[69] Chiu, Y., Levandier, D., Austin, B., Dressler Rainer, A., Murray, P. T., Lozano, P. and Martinez-Sanchez, M. "Mass Spectrometric Analysis of Ion-Emission from Selected Colloid Thruster Fuels," *39th AIAA/ASME/SAE/ASEE Joint Propulsion Conference and Exhibit*. AIAA, Huntsville, Al, 2003.
[70] Ticknor, B. W., Miller, S.W., and Chiu, Y.H. "Mass Spectrometric Analysis of the Electrospray Plume from an Externally Wetted Tungsten Ribbon Emitter," *45th AIAA/ASME/SAE/ASEE Joint Propulsion Conference & Exhibit*. Denver, Colorado, 2009.
[71] Chiu, Y. H., Austin, B.L., Dressler, R.A., Levandier, D., Murray, P.T., Lozano, P., and Martinez-Sanchez, M. "Mass Spectrometric Analysis of Colloid Thruster Ion Emission from Selected Propellants," *Journal of Propulsion and Power* Vol. 21, No. 3, 2005, pp. 416-423.
[72] de la Mora, J. F., and Loscertales, I. G. "The current emitted by highly conducting Taylor cones," *Journal of Fluid Mechanics* Vol. 260, No. special issue, 1994, pp. 155-184. doi: 10.1017/S0022112094003472
[73] Lozano, P. "Studies on the Ion-Droplet Mixed Regime in Colloid Thrusters." Massachusetts institute of Technology, 2003.
[74] Chiu, Y. H., Gaeta, G., Levandier, D. J., Dressler, R. A., and Boatz, J. A. "Vacuum electrospray ionization study of the ionic liquid, [Emim][Im]," *International Journal of Mass Spectrometry* Vol. 265, No. 2-3, 2007, pp. 146-158. doi: 10.1016/j.ijms.2007.02.010
[75] Gamero-Castano, M. "The structure of electrospray beams in vacuum," *Journal of Fluid Mechanics* Vol. 604, 2007, pp. 339-368.
[76] Prince, B. D., Fritz, B. A., and Chiu, Y.-H. "Ionic Liquids in Electrospray Propulsion Systems," *Ionic Liquids: Science and Applications*. Vol. 1117, American Chemical Society, 2012, pp. 27-49.
[77] Politi, L., Morini, L., Groppi, A., Poloni, V., Pozzi, F., and Polettini, A. "Direct determination of the ethanol metabolites ethyl glucuronide and ethyl sulfate in urine by liquid chromatography/ electrospray tandem mass spectrometry," *Rapid Communications in Mass Spectrometry* Vol. 19, 2005, pp. 1321-1331.
[78] Courtney, D. G., and Shea, H. "Fragmentation in Time-of-Flight Spectrometry-Based Calculations of Ionic Electrospray Thruster Performance," *Journal of Propulsion and Power* Vol. 31, No. 5, 2015, pp. 1500-1504. doi: 10.2514/1.B35837

[79] Miller, C., and Lozano, P. C. "Measurement of the Fragmentation Rates of Solvated Ions in Ion Electrospray Thrusters," *52nd AIAA/SAE/ASEE Joint Propulsion Conference*. American Institute of Aeronautics and Astronautics, Salt Lake City, UT, 2016.
[80] Stein, S. E. *Mass Spectra*. Gaithersburg MD, 20899: National Institute of Standards and Technology.